

# EVOLUTION OF LOCAL STRUCTURES IN ALKALI-BORATE GLASSES

Richard Kerner\*, Dina Maria dos Santos-Loff\*\* and Ana Cristina Rosa\*\*

\* Address : LPTMC, Sorbonne-Université - CNRS UMR 7600 ,  
Tour 13-23, 5-ème , Boite 121, 4 Place Jussieu, 75005 Paris, France  
Tel.: +33 1 44 27 72 98, Fax: +33 1 44 27 51 00,  
email : richard@kerner@sorbonne-universite.fr

\*\* Address: Departamento de Matemática, Universidade de Coimbra,  
3000 Coimbra, Portugal (retired).  
e-mail dina@mat.uc.pt, e-mail cristina@mat.uc.pt

## Abstract

We analyze the dependence of relative proportion of various characteristic clusters in binary alkali-borate glasses on modifier's concentration  $x$ . A pure  $B_2O_3$  glass contains a huge amount of boroxol rings and some amount of boron atoms in between, linking the boroxol rings via oxygen bonds. The addition of the  $Na_2O$  modifier creates four-coordinated borons, but the resulting network glass remains totally connected. We study local transformations that lead to creation of new configurations like *tetraborates*, *pentaborates*, *diborates*, etc., and set forth a non-linear differential system similar to the Lotka-Volterra model. The resulting density curves of various local configurations as functions of  $x$  are obtained. Then the average rigidity is evaluated, enabling us to compute the glass transition temperature  $T_g(x)$  for a given value of  $x$

# 1 Introduction

In this article we present a structural analysis of amorphous network formed by the boron oxide  $B_2O_3$  with addition of an alkali modifier  $Na_2O$ . Our approach is exploiting two essential features of this network: *connectivity* and *rigidity*. Both characteristics can be given a quantitative treatment, and serve as essential parameters determining physical properties of alkali-borate glass  $(B_2O_3)_{(1-x)}(Na_2O)_x$ .

The alkali borate glasses,  $(1-x)B_2O_3+xNa_2O$  or  $(1-x)B_2O_3+xLi_2O$  are well known and present an interesting field for theoretical modelling. Typical *structural glasses*, their physical properties are determined by topological and geometrical features characterizing medium-range order. Therefore the statistical approach, dealing with *probabilities* of finding a given local configuration, remains the most appropriate methodology. Mathematical models exploring structural properties of alkali-borate glasses were initiated since the early eighties ([1], [2], [3]) The most important development resulted from the collaboration with the experimentalists. M. Balkanski and M. Massot ([4]) The final version of the model, including the stochastic matrix approach, was elaborated by R.K and D.M. dos Santos-Loff, with R.A. Barrio, M. Micolaut, G. G. Naumis and J.-P. Duruisseau (see e.g. [5], [6], [7]).

In those models we used the stochastic matrix method combined with analysis of energy costs of forming particular local configurations. The entropy was accounted for via average connectivity and coordination number. The model was focussed on glass transition temperature  $T_g$  and gave fair predictions concerning the dependence of  $T_g$  on modifier concentration in alkali-borate glasses in particular ([8], [9]) The present paper deals with a more detailed analysis of stable local structures appearing in alkali borate glasses, whose presence was corroborated by many data obtained via Raman or NMR spectroscopy. The “breathing mode” identified as the  $808^{-1}$  cm line in the Raman spectrum is a firmly identified signature of boroxol rings ([11], [1], [14], [3]).

Here we derive a system of differential equations of Lotka-Volterra type, describing the evolution of probabilities of various local structures as functions of alkali modifier’s molar concentration. This enables us to evaluate the average rigidity defect  $\langle r \rangle$  for a given alkali concentration  $x$ , and introduce a simple model of glass transition temperature dependence on  $\langle r \rangle = \langle r \rangle(x)$  akin to the Gibbs-Di Marzio formula (see [13]).

## 2 Local structures in amorphous $B_2O_3$

A pure  $B_2O_3$  glass is an amorphous solid in which atoms form a typical random network with covalent bonds. However, taking into account that boron atoms are three-coordinated, and that all oxygen atoms form bonds between them, one cannot produce a random network in three dimensions without forming rings. In both crystalline and amorphous  $SiO_2$  the network contains mostly the 6-folded rings; in amorphous  $B_2O_3$  the 3-fold rings dominate (see e.g. [11], [12], [15], [16], [3], [8]).

In the case of the  $B_2O_3$  glass we admit that the boroxol rings are the most common structure, which does not exclude the existence of much bigger closed circuits, which however do not have any particular physical signature. The “breathing mode” identified as the  $808^{-1}$  cm line in the Raman spectrum is a firmly identified signature of boroxol rings ([1], [14]).

The structure of random  $B_2O_3$  network must therefore contain lots of boroxol rings as well as certain amount of isolated boron tripods  $B(O_{\frac{1}{2}})_3$ :

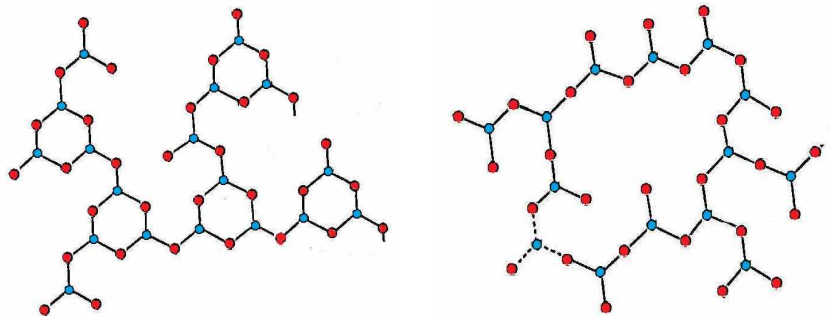


Figure 1: A fragment of random  $B_2O_3$  network: Left: with boroxol rings, Right: without boroxol rings. Boron atoms are blue, oxygens are red.

Larger units should include boroxol rings. Our aim is to include medium-range configurations containing enough information about the boroxol ring content of the network. There were a lot of discussions concerning short-range local structure of amorphous  $B_2O_3$ . The most controversial point was the very existence and possible rate of the *boroxol rings*, represented in (1).

The relative abundance of boroxol rings has been the subject of many discussions. Certain estimates, both theoretical and experimental, including computer simulations, converge to the value  $f \simeq 0.75$  for the relative part of boron atoms belonging to boroxol rings versus the total number of boron

atoms in the structure. ([23]) The lower limit seems to be that of  $f = 0.5$ , as advocated by Wright and Vedishcheva in [19]

Some authors claim an even more massive presence of boroxol rings, corresponding to  $f \simeq 0.83$  ([5], [6]), which may be considered the upper limit for  $f$ . The models with low values of  $f$  seem to be gradually dismissed by most of the authors. In what follows, we will admit the value of  $f = 0.83$ , conformal to our model in ([5] and [14]) i.e. slightly more than 80% of all boron atoms in pure  $B_2O_3$  glass are contained in boroxol rings. Of course, this supposes an ideal case, when the glass is annealed very slowly letting the most homogeneous and energetically and entropically privileged configuration to be realized; rapid quenching may lead to totally different results, similar to a frozen structureless liquid.

The entire network can be subdivided now into  $N_R$  boroxol rings  $R$  and some number of isolated borons,  $N_I$ . The relative probabilities to find a ring or an isolated boron are therefore

$$p_R = \frac{N_R}{N_R + N_I} \quad \text{and} \quad p_I = \frac{N_I}{N_R + N_I}, \quad p_R + p_I = 1. \quad (1)$$

Let us denote the part of boron atoms contained in boroxol rings by  $\xi$ ; this parameter can be expressed by  $p_R$  via simple relation:

$$\xi = \frac{3p_R}{3p_R + p_I}, \quad p_R = \frac{\xi}{3 - 2\xi}. \quad (2)$$

For example,  $p_R = p_I = 1/2$  as supposed by Wright and Vedishcheva in [19], will correspond to  $\xi = 0.75$ , which is the value advocated by Ferlat et al. (see [23]). However, with such a high amount of “free” borons non contained in boroxol rings chains of two or even three such entities would appear, conveying extra floppiness and inhomogeneity to the network. In our model based on the stochastic agglomeration (see [2], [5] and [6]) and using the binding energies conjectured in ([11]), we arrive to the value 83% of boron atoms trapped in boroxol rings, too.

It is easy to derive the relative frequency of  $A$  and  $B$  configurations in an amorphous  $B_2O_3$  network. Let the probability to find an  $A$ -configuration be  $p_A$ , and that of the  $B$  configuration  $(1 - p_A)$ . Then we should have:

$$\frac{3}{4}p_A + (1 - p_A) = 0.83, \quad (3)$$

which yields the result  $p_A = 0.68$ , close enough to 66,67% to enable us to use the simplest fraction available, and assume the presence of 2/3 of clusters  $A$

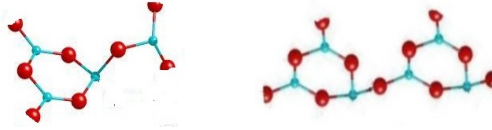


Figure 2: Two typical clusters, named A and B, made with boroxol rings and free boron tripods. Note that they have the same exterior connectivity: 4.

and 1/3 of clusters  $B$  in the network. By the way, replacing 0.68 by  $2/3$  in 3 would change the value 0.83 into  $\frac{3}{4} \cdot \frac{2}{3} + \frac{1}{3} = 0.83333$ , a negligible variation, below the experimental precision.

### 3 Connectivity and rigidity

The chemical bonds in  $B_2O_3$  glass belong to the category of *covalent bonds*, whereas the  $Na$  atoms are linked to oxygen atoms via *ionic* bonding ([17], [1]). In binary  $(1-x)B_2O_3+xNa_2O$  glasses local structures are made of atoms strongly connected through covalent bonds, and ions  $Na^+$  loosely connected to the main network when they stick to boron atoms, creating extra oxygen bond, or more strongly connected to oxygen atoms, breaking bonds between neighboring borons and creating dangling oxygen bonds. The first tendency prevails at low concentrations, while the second possibility is realized at molar  $Na_2O$  concentrations higher than 35%.

Considering the network just as a collection of isolated atoms  $B$ ,  $O$  and  $Na$  does not give any structural information beyond its pure chemical content. The subdivision of random network into molecules still does not give enough information, in particular, about the local ring structure.

Adding alkali modifier creates new local configurations. The molecules of  $Na_2O$  dissociate in the hot melt, and the  $Na^+$  ions come close to the boron atoms of the network, thus creating a new oxygen bond and transforming three-coordinate boron atoms into four-coordinate ones, at least at concentrations not higher than 25% as shown in the following figure:

We see that the rate of  $B_4$  atoms steadily grows until  $x$  reaches about 0.4, then starts to decrease. This is due to the fact that if throughout the process of consecutive modifier addition the connectivity has to be maintained, i.e. no dangling bonds are being created. But even if all boron atoms were transformed into four-coordinated  $B_4$  complexes, this will saturate at  $x = 0.5$ .

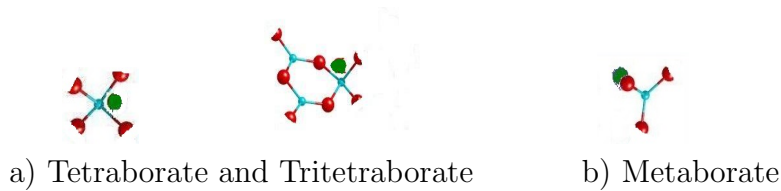


Figure 3: Examples of positioning of an  $Na^+$  ion

Beyond, another way of inserting the  $Na^+$  ions takes progressively place, the breaking of oxygen bonds between the borons and forming oxygens saturated with  $Na^+$ , i.e. dangling oxygens. The boron atoms with such a saturated bond become in fact two-coordinate, so that the overall connectivity remains maintained. The figure below displays two processes resulting from addition of the  $Na_2O$  modifier:

- Transforming a three-valenced boron into  $B_4$  tetra-coordinate unit with an extra oxygen bond; local connectivity increases
- Creating a non-bridging oxygen, i.e. breaking an oxygen bond; the connectivity decreases.

The result is measurable with NMR techniques; the relative amount of 4-valenced borons is displayed on the left in Figure below. It is noticeable that the glass transition temperature varies in a similar manner, as shown on the right. We discuss the dependence of  $T_g$  on  $x$  later on, in Sect. 6.

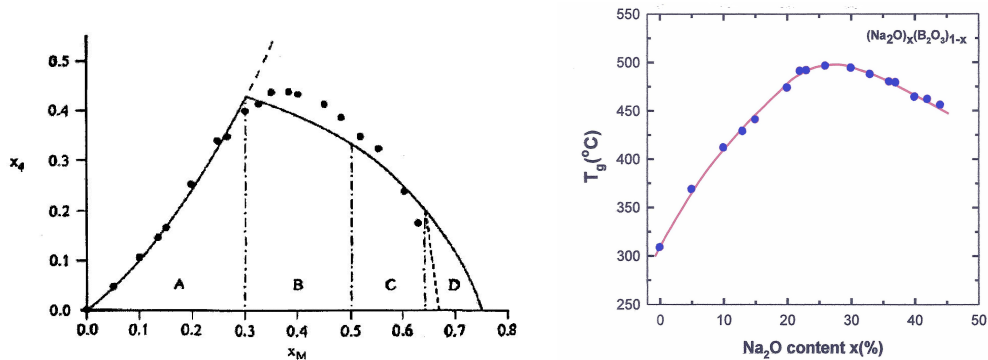


Figure 4: Left: the rate of four-coordinate borons ( $x_4$ ) with a  $Na^+$  ion and an extra oxygen bond as a function of modifier density  $x_M$  (after A.Wright et al., 1997); Right:  $(Na_2O)_x(B_2O_3)_{1-x}$  glass transition temperature  $T_g$  as function of  $x$  (after Vignobooran and Boolchand))

We observe that the rate of  $B_4$  atoms steadily grows until  $x$  reaches about 0.4, then starts to decrease. This is due to the fact that if throughout the process of consecutive modifier addition the connectivity has to be maintained, i.e. no dangling bonds are being created.

Let us now proceed to a systematic display of clusters containing the  $Na^+$  ions. We shall look firstly for clusters with four external bonds, so that they can replace the configurations  $A$  and  $B$  with no connectivity change in the network, and without creating dangling bonds.

The calculus of the average modifier content  $x$  in each local configuration is easy, and will be given in each particular case.

Besides, In each case, we shall proceed to the calculus of another important parameter, the *rigidity* of each configuration displayed. The latter is defined as the difference between the mean value of the number of degrees of freedom per atom  $N_f$  and the “free” value 3,  $r = N_f - 3$ .

If  $r < 0$ , the cluster is *floppy* or *underconstrained*;

If  $r = 0$ , the cluster is *isostatic*;

If  $r > 0$ , the cluster is *rigid* or *overconstrained*.

The calculus of rigidity of given configuration is based on the following assumptions concerning both *angular* and *stretching* constraints:

- Each three-coordinated boron atom,  $B_3$  creates 3 angular constraints (bond angles =  $120^\circ$ );
- Each tetra-coordinated boron atom,  $B_4$ , (with an extra oxygen bond) creates 5 angular constraints;
- An oxygen atom inside a boroxol ring creates 1 angular constraint, whereas oxygen bonds out of rings have their angular constraints broken;
- All covalent bonds without exception are equivalent to 1 bond-stretching constraint; finally, the  $Na^+$  ions are not taken into account in the rigidity calculus, their position not being strictly defined.

As an example; let us evaluate the rigidity of clusters  $A$  and  $B$ . In the first case (see 2) we have 4 three-coordinate boron atoms, contributing  $4 \times 3 = 12$  angular constraints, and three oxygens contained in the boroxol ring, thus contributing  $3 \times 1 = 3$  angular constraints. The bridging oxygen relying the boroxol ring with the isolated 3-coordinate boron is supposed not to contribute to angular constraints. The linear (stretching) constraints are equal to the number of covalent bonds, here 12, giving the total number of constraints equal  $N_c = 27$ . The number of atoms involved in the  $A$ -configuration is  $N_a = 10$  - four “halves” of bonding oxygens plus four borons and four

oxygens. Dividing  $N_c$  by  $N_a$  we get the average number of constraints per atom equal to 2.7, which is 0.3 short of 3.0 which defines an *isostatic* configuration. Therefore the *A*-clusters are *floppy*, (or underconstrained), with  $r = (N_c/N_a) - 3 = -0.3$ .

A similar calculus yields  $N_c = 42$ ,  $N_a = 15$ ,  $r = (42/15) - 3 = -0.2$ . The *B*-cluster is also floppy, albeit a bit less than its *A* counterpart.

In what follows, we use the classification and names of particular local clusters containing one or more sodium ions as given by Wright *et al* in ([25]). Here are the structural units with one  $Na^+$  ion, and with the same total connectivity (coordination number = 4) as the original clusters *A* and *B*: Adding more of  $Na_2O$  leads to the multiplication of valences. To keep

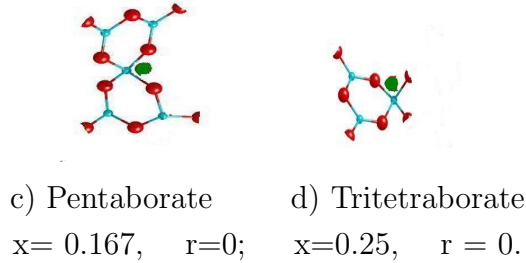


Figure 5: Two important clusters with one  $Na^+$  ion; both are isostatic.

the connectivity balance, some  $Na^+$  ions break oxygen bonds and remain in the vicinity of one of the oxygens.

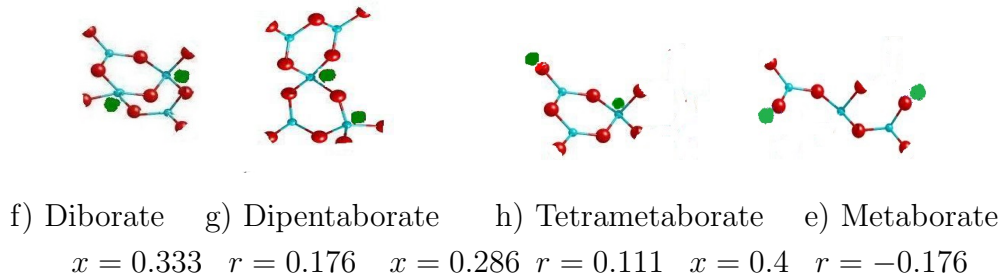


Figure 6: Diborate (left) and two other clusters with two  $Na^+$  ions. The total connectivity is still  $5 + 3 = 8$

The clusters with two  $Na^+$  ions are: a *diborate* with connectivity 4, and two new configurations with modified connectivity, 5 and 3, *Di-pentaborate*



and *Trimetaborate*. In order for connectivity being conserved, the 3- and 5-coordinate entities must appear in equal numbers.

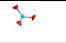
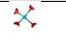
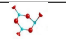
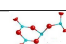
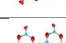
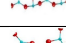
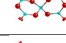
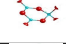
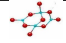
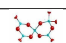
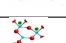
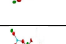
Name	Symbol	$B_4$ -content	alkali $x_M$	Rigidity $r$
Single B3		0	0	-0.6
Single B4		1	0.5	0
Boroxol ring		0	0	-0.2
A-cluster		0	0	-0.3
B-cluster		0	0	-0.173
Pentaborate		0.2	+0.167	0
Tritetaborate		0.333	0.25	0
Diborate		0.5	0.333	+0.182
Dipentaborate		0.4	0.286	+0.111
Ditritetaborate		0.667	0.4	+0.176
Metatriborate		0.333	0.4	-0.176
Metaborate		0	0.4	-0.882

Table 1. Main local structures in alkali-borate glasses

When the concentration of  $Na_2O$  gets close to 40%, new clusters are formed, containing three  $Na^+$  ions, with connectivity up to 6 and the the *pyroborate* clusters containing three  $Na^+$  ions, with connectivity 2, but we shall not consider them here, restricting the range of  $x$  below the  $x = 0.35$  limit. Now we are able to define minimal sets of pure  $B_2O_3$  clusters which can transform into new clusters containing the  $Na^+$  ions in such a way that the overall connectivity remains unchanged.

## 4 Transforming clusters with alkali modifier

According to the hypothesis exposed in Sect. 2 and corroborated by numerous experimental data, a pure  $B_2O_3$  melt about to undergo a glass transition contains boroxol rings and isolated borons so that the amount of boron atoms trapped in 3-fold boroxol rings amounts to 83%. After slow annealing, the resulting amorphous glassy network can be subdivided into  $A$  and  $B$  local clusters each with exterior connectivity 4, in proportion 2 to 1, i.e. 67% of  $A$ 's and 33% of  $B$ 's.

Now suppose that a small amount of alkali modifier, say  $Na_2O$  for example, is added to the melt, transforming a pure  $B_2O_3$  into a glassy network containing certain amount of four-coordinate borons  $B_4$  due to the disruptive action of the  $Na^+$  ions. If the connectivity of the resulting network is to be maintained, this means that some number of local structures  $A$  and  $B$  had to be replaced by four-coordinate clusters containing  $B_4$  borons created by the  $Na^+$  ions. In what follows, we shall consider the  $Na_2O$  molecules dissolving into the melt and creating TWO local clusters with one  $Na^+$  ion (i.e. with only one  $B_4$  tetraborate each), supposing that no clusters with two or more  $Na^+$  ions can be spontaneously created at the onset of the alkali oxide dissolving in the pure boron oxide melt. This requires in turn considering two local clusters at once, which may be two  $A$ 's, an  $A$  and a  $B$ , or two  $B$ 's; in each case, the total external connectivity is  $2 \times 4 = 8$ , and the modified  $Na^+$  containing clusters should display the same connectivity.

It should be made clear that these transformations of local structures should not be taken literally, like a genuine chemical reaction. The two dissolved  $Na^+$  and extra oxygen  $O^{--}$  ions sneak their way into the network perhaps in a complicated and chaotic manner, but at the end of the day the result can be expressed as a substitution of a pair of pure  $B_2O_3$  clusters by  $Na^+$  enriched ones, with strict connectivity conservation.

While comparing many possible transformations of this sort, we shall try to minimize the rigidity variation and maximize the homogeneity of the resulting local structures.

Let us show how the molecules of  $Na_2O$  can be inserted into the network with local connectivity remaining conserved. The first “reaction” can be represented as follows: Another reaction involving  $A$  and  $B$  clusters is shown

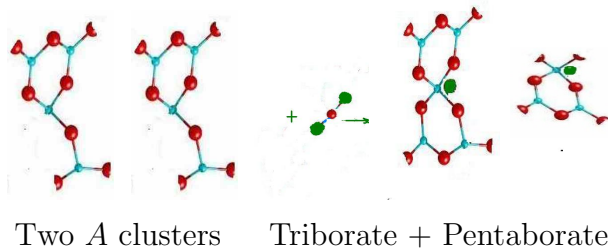


Figure 7: Insertion of one  $Na_2O$  molecule into a pure amorphous  $B_2O_3$  network. The transformation can be encoded as  $2A + Na_2O \rightarrow P + T$ .

below: Finally, there is another reaction involving one extra  $Na_2O$  molecule

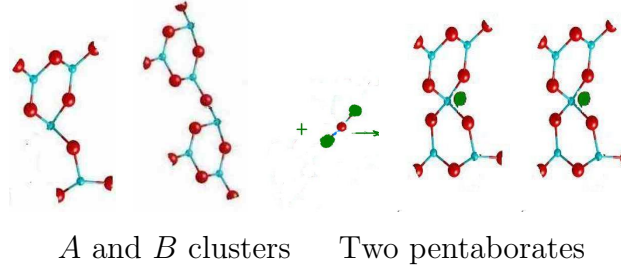


Figure 8: Insertion of one  $Na_2O$  molecule into a pure amorphous  $B_2O_3$  network. The transformation can be encoded as  $A + B + Na_2O \rightarrow 2P$ .

with local connectivity conservation, involving two  $B$  clusters:

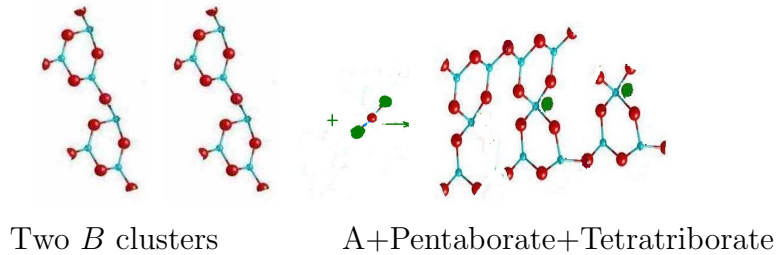


Figure 9: Insertion of one  $Na_2O$  molecule into a pure amorphous  $B_2O_3$  network. This transformation can be encoded as  $2B + Na_2O \rightarrow P + T + A$ .

The three “reactions” shown in Figures (7, 8 and 9) above do in fact exhaust all possibilities of insertion of a  $Na_2O$  molecule in the  $B_2O_3$  network with consequent disappearance of  $A$  and  $B$  clusters transformed into  $P$ ’s and  $T$ ’s (pentaborates and tetratriborates), with a little amount of  $A$  clusters still remaining.

At this point it is worthwhile to evaluate the relative production rate of pentaborates and tetratriborates, which are dominant at the first stages of alkali modifier’s addition to the network. A given reaction’s rate is proportional to the probability of picking up an appropriate couple of clusters,  $A + A$ ,  $A + B$  or  $B + B$ , as shown in Figures (7, 8 and 9).

$$p_P \sim 1 \cdot p_A^2 + 2 \times 2p_A p_B + 1 \cdot p_B^2, \quad p_T \sim 1 \cdot p_A^2 + 1 \cdot p_B^2, \quad p_A \sim 1 \cdot p_B^2. \quad (4)$$

Inserting the initial rates of  $A$  and  $B$  clusters (i.e.  $\binom{0}{p}_A = 2/3$ ,  $\binom{0}{p}_B = 1/3$ ),

we get the following linear approximation:

$${}^{(1)}p_P \sim \frac{4}{9} + \frac{8}{9} + \frac{1}{9}, \quad {}^{(1)}p_T \sim \frac{4}{9} + \frac{1}{9}, \quad {}^{(1)}p_A \sim \frac{1}{9}. \quad (5)$$

Next reactions resulting from inserting more  $Na_2O$  molecules, with local connectivity conservation maintained:

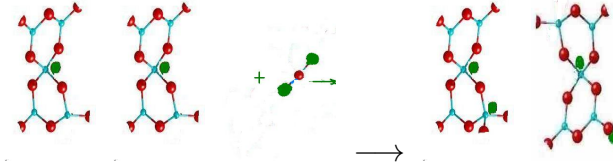
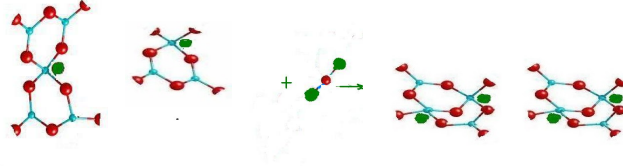


Figure 10: Insertion of one  $Na_2O$  molecule into a low alkali ( $x \leq 18\%$ ) amorphous  $B_2O_3$  network. This transformation can be encoded as  $2P + Na_2O \rightarrow DP + MP$ .



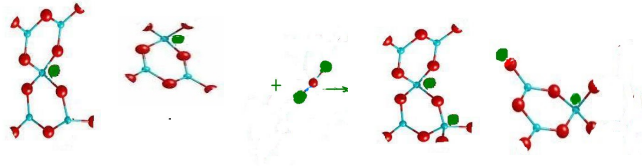
Pentaborate + Tritetaborate      Two Diborates

Figure 11: Insertion of one  $Na_2O$  molecule into a pure amorphous  $B_2O_3$  network. This transformation can be encoded as  $P + T + Na_2O \rightarrow 2D$ .

An alternative issue of the same “reaction” can be also envisaged, producing new configurations, a di-pentaborate and a meta-tetaborate, with respective connectivities 5 and 3 instead of 4 plus 4 in the case of two diborates:

The Raman spectral analysis and NMR experiments have led to quite a precise picture of evolution of numbers of various local configurations with continuous increase of the  $Na_2O$  modifier content.

The variation of abundance of local configurations is shown in the following figure:



Pentaborate + Tritetaborate      Dipentaborate and Tetrametaborate

Figure 12: Insertion of one  $Na_2O$  molecule into a low alkali content ( $x \leq 18\%$ ) borate glass network. This transformation can be encoded as  $P + T + Na_2O \rightarrow DP + MT$ .

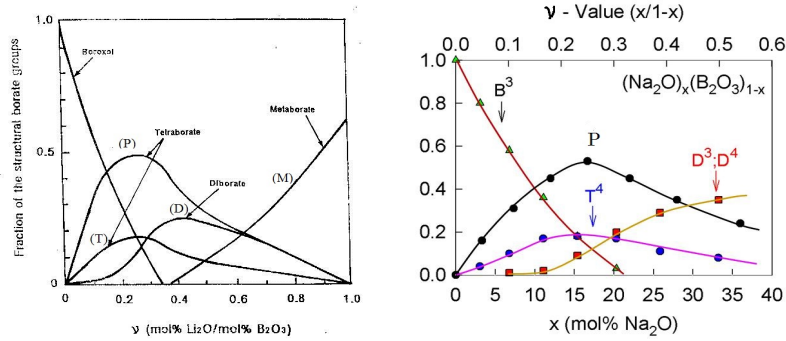


Figure 13: Abundance of main alkali-borate local configurations as function of modifier's molar density  $x$ . Left:  $(1-x)B_2O_3 + xLi_2O$ , due to M. Balkanski and M. Massot; Right:  $(1-x)B_2O_3 + xNa_2O$ , courtesy of P. Boolchand.

## 5 The Volterra approach

The evolution of various "species" of boroxol clusters with progressive addition of an alkali modifier is similar to the evolution of biological systems with different living organisms, competing for food and space, or even eating each other (predators and preys).

The simplest model is given by two species only, the prey  $x$  and the predator  $y$ . The evolution of their (relative) numbers can be described as follows:

The prey population  $x(t)$  increases at a rate  $Axdt$ , proportional to its own number, but is simultaneously killed by predators at a rate  $-Bxydt$ ;

The predator population  $y(t)$  decreases at a rate  $-Cydt$ , proportional to its own number, but increases at a rate  $Dxydt$ ; which leads to the following

differential system:

$$\frac{dx}{dt} = Ax - Bxy, \quad \frac{dy}{dt} = -Cy + Dxy.$$

A typical solution of this system displays a neat quasi-periodic character: when rabbits proliferate, so do the foxes, which chase rabbits whose population decreases, thus condemning foxes to starve from hunger; this in turn gives the rabbits more possibility to proliferate, and so on (see e.g. Kerner-book

We shall apply similar method to the “evolution” of abundances of various types of local configurations (introduced in the previous section and labeled  $A, B, TT, P, D$ , etc.) with growing modifier concentration  $x$ , which variable will replace time in Lotka-Volterra differential system.

The evolution of relative number of local configurations can be described in a similar manner. The time parameter of the biological model is replaced here by the modifier concentration  $x$ .

In order to establish the system of differential equations of Lotka-Volterra type, let us analyze what happens to the network when a small amount of modifier,  $\Delta n$  molecules, is added to the network, the constraint being connectivity conservation.

Let us add a small number of molecules  $\Delta n$ . to a network containing  $N$  clusters of types  $A, B, P, TT, D, M$  etc., their respective numbers being  $N_A, N_B, N_P, N_{TT}, N_D, N_M$ , etc.

In order to make the explanation of our model as clear as possible, let us start with only first five configurations present,  $A, B, P, TT$  and  $D$ . Notice that even if all local configurations ended up as being transformed into diborates ( $D$ ), the concentration  $x$  could not bypass the mark  $x = 0.33$ . Beyond that concentration new local configurations appear, the Di-Tetraborates ( $x = 0.4$ ), Tri-Pentaborates ( $x = 0.375$ ), Di-Metaborates and Tri-Metaborates ( $x = 0.5$ ), which we shall not take into account in the simplified version of the model, valid only for  $x$  below 0.35 at most.

Let us suppose then that at a given concentration  $x$  of the  $Na_2O$  alkali modifier, the sample glass obtained by annealing from melt contains  $N$  molecules of the glass former  $B_2O_3$  and  $n$  molecules of the modifier  $Na_2O$ . The relative concentration is

$$x = \frac{n}{N + n}. \quad (6)$$

Sometimes the ratio  $\nu$  of  $Na_2O$  molecules to the  $B_2O_3$  molecules is used, and one has the obvious relation between these two parameters,

$$\nu = \frac{n}{N}, \quad \nu = \frac{x}{1-x}, \quad x = \frac{\nu}{1+\nu}. \quad (7)$$

At the same time, the numbers of specific local configurations are:

$$N_A, N_B, N_{TT}, N_P \text{ and } N_D.$$

Let us denote the sum of all these numbers by  $N_{tot}$ ; then we can define the probabilities of finding at random one of the five local configurations as follows:

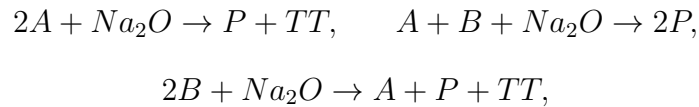
$$p_A = \frac{N_A}{N_{tot}}, \quad p_B = \frac{N_B}{N_{tot}}, \quad p_{TT} = \frac{N_{TT}}{N_{tot}}, \quad p_P = \frac{N_P}{N_{tot}}, \quad p_D = \frac{N_D}{N_{tot}}; \quad (8)$$

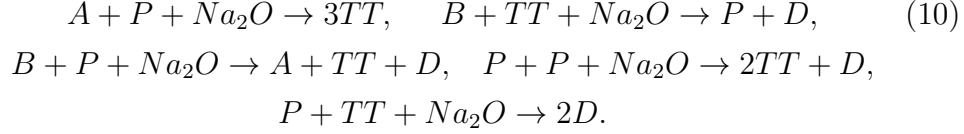
Their sum is equal 1 as it should be for the probabilities; this is why only four functions out of five are independent. At the same time, the total number of  $B_2O_2$  molecules in the sample can be found according to the obvious formula

$$N = 2p_A + 3p_B + \frac{3}{2}p_{TT} + \frac{5}{2}p_P + 2p_D. \quad (9)$$

In order to establish the differential system for the unknown functions  $p_A(x)$ ,  $p_B(x)$ ,  $p_{TT}(x)$ ,  $p_P(x)$  (the function  $p_D(x)$  can be found then from the normalization relation (4)), we must compare the numbers of the same configurations after addition of some small amount of modifier in the form of  $\Delta n$  new molecules of  $Na_2O$  dissolved in the former melt and annealed to form a new glass. For this, we have to decide what particular changes have occurred in the distribution of local clusters after the adjunction of new alkali molecules. It is enough to know the fate of one molecule of  $Na_2O$  dissociated in the melt, and evaluate the probabilities of various issues, then multiplying these probabilities by  $\Delta n$ .

We have found the following reactions involving one  $Na_2O$  molecule, leaving the total connectivity of new clusters exactly the same as the initial ones. Here is the summary of all such transformations leading to new local configurations:





In the list of admissible connectivity-preserving transformations we have tacitly admitted the principle according to which local configurations containing alkali ions are formed progressively: the alkali-rich ones, containing two or more  $Na^+$  ions, are formed only after most of the network has been transformed into configurations with one  $Na^+$  ion only. As a matter of fact, a reaction consisting in transformation of cluster  $A$  with four boron atoms into a diborate  $D$  with four boron atoms and two  $Na^+$  ions is theoretically possible, because it also conserves the connectivity (4), but we consider its probability close to zero.

The combination  $TT + TT$  with addition of a molecule of  $Na_2O$  can lead to configuration conserving global connectivity only if one introduces new configurations with less than four external bonds, i.e. metaborates; at this stage we shall not count them in, stopping the alkali concentration below  $x = 0.3$ , say.

It follows from the above transformations (10) that a combination of one  $Na_2O$  molecule with two  $A$ -configurations transforms them in a pair  $TT + P$  (a tri-tetraborate plus a pentaborate), i.e. one  $Na_2O$  molecule leads to the destruction of two  $A$  clusters and the creation of one  $TT$  and one  $P$  cluster. The resulting variation of corresponding total numbers of each of the species taking part in the transformation is

$$\Delta N_A = -2, \quad \Delta N_{TT} = +1, \quad \Delta N_P = +1.$$

The probability of such issue is proportional to the product of probabilities of picking at random one  $A$ -cluster, i.e.  $p_A^2$ . Although there could be certain differences between the energy barriers which may be different for particular transformations, at present stage we shall not take them into account, assuming that the dominant feature and driving forces for transformations are the *connectivity* and *homogeneity* of the resulting network. The result of the first reaction after the addition of  $\Delta n$  alkali molecules is then

$$\Delta N_A \sim -2p_A^2 \Delta n, \quad \Delta N_{TT} \sim +p_A^2 \Delta n, \quad \Delta N_P \sim +p_A^2 \Delta n, \quad (11)$$

all other configuration numbers remaining unchanged by this reaction. Similarly, from the second reaction of (10) we get the following variations:

$$\Delta N_A \sim -2p_{APB} \Delta n, \quad \Delta N_B \sim -2p_{APB} \Delta n, \quad \Delta N_P \sim +4p_{APB} \Delta n. \quad (12)$$



The probability of an encounter of two different configurations  $A$  and  $B$  is proportional to  $2p_A p_B$ ; there is only one  $A$  and one  $B$  destroyed, but two  $P$ 's created, whence from the factor 4 in the last expression. Note also that in both cases the sum of all variations is zero; this is because there are as many destroyed entities as the created ones, and the sum of all probabilities remains normalized to one in the initial as well as in the final state.

The situation is a bit different with the third reaction of (10), because *three* new configurations are created instead of the two ones ( $B + B$ ) that have disappeared. In order to keep the sum of the contributions null, normalizing factor  $2/3$  has to be introduced on the right hand side, because we are comparing the initial probabilities related to *two* items with the final probabilities related to *three* new items. This yields the following account of the result of the third reaction in (10):

$$\Delta N_A \sim \frac{2}{3} p_B^2 \Delta n, \quad \Delta N_B \sim -2 p_B^2 \Delta n, \quad \Delta N_{TT} \sim \frac{2}{3} p_B^2 \Delta n, \quad \Delta N_P \sim \frac{2}{3} p_B^2 \Delta n. \quad (13)$$

With this in mind we can now evaluate and sum up the contributions coming from all the reactions given in (10), arriving at the following result:

$$\begin{aligned} \Delta N_A &= \left( -2p_A^2 - 2p_{APB} - 2p_{APT T} - 2p_{APP} + \frac{2}{3} p_B^2 + \frac{2}{3} 2p_{BPP} \right) \Delta n, \\ \Delta N_B &= \left( -2p_{APB} - 2p_B^2 - 2p_{BPT T} - 2p_{BPP} \right) \Delta n, \\ \Delta N_{TT} &= \left( p_A^2 + \frac{2}{3} (p_B^2 + 3 \times 2p_{APP} + 2p_{BPP} + 2p_P^2) - 2p_{BPT T} - 2p_{PPT T} \right) \Delta n, \\ \Delta N_P &= \left( p_A^2 + 4p_{APB} + \frac{2}{3} p_B^2 + 2p_{BPT T} - 2p_{APP} - 2p_{BPP} - 2p_P^2 - 2p_{PPT T} \right) \Delta n, \\ \Delta N_D &= \left( 2p_{APT T} + 2p_{BPT T} + 4p_{PPT T} + \frac{2}{3} (2p_{BPP} + p_P^2) \right) \Delta n. \end{aligned} \quad (14)$$

One easily checks that the sum of all left-hand sides is zero, which means that only four of the above five equations (14) are linearly independent.

Before passing to the continuous limit and form differential equations, let us express everything exclusively in terms of probabilities and the unique independent variable, the modifier's molecular content  $x$ . In order to change from  $\Delta N = a$ ,  $\Delta N_B$ , etc., into  $\Delta p_A$ ,  $\Delta p_B$ , etc., it is enough just to divide both sides by the total number of configurations. As usually in differential calculus, the  $\Delta N_i$  and  $\Delta n$  are treated as infinitesimals, so there is no difference which actual values of  $N_{tot}$  are chosen, the initial or the final ones.

Still, we have to express the ratio  $\Delta n/N_{tot}$  in terms of the differential  $\Delta x$ . At the moment, on the right-hand side we have got the ratio  $\Delta n/N_{total}$ ; but this can be easily transformed into the quantity  $\Delta \nu$  as follows. Remember that there is a simple relationship between  $N_{tot}$  given in (9); therefore, dividing both sides by  $N_{tot}$ ; we get, by definition of configuration probabilities,

$$\frac{N}{N_{tot}} = 2p_A + 3p_B + \frac{3}{2}p_{TT} + \frac{5}{2}p_P + 2p_D = \langle k \rangle, \quad (15)$$

where we note by  $\langle k \rangle$  the *average number of  $B_2O_3$  molecules* per local configuration, so that one can write

$$N = \langle k \rangle N_{tot}, \quad \text{so that} \quad \frac{\Delta n}{N_{tot}} = \langle k \rangle \frac{\Delta n}{N} = \langle k \rangle \Delta \nu. \quad (16)$$

Now we can proceed to the continuous limit, dividing by  $\Delta \nu$  both sides of the equations (14). As an example, let us write down the first of the five equations:

$$\frac{dp_A}{d\nu} = \langle k \rangle \left( -2p_A^2 - 2p_{APB} - 2p_{APT} - 2p_{APP} + \frac{2}{3}p_B^2 + \frac{2}{3}2p_{BPP} \right), \quad (17)$$

and we remind that  $\langle k \rangle = 2p_A + 3p_B + \frac{3}{2}p_{TT} + \frac{5}{2}p_P + 2p_D$ . The derivation with respect to the variable  $\nu$  can be transformed into the derivation with respect to the variable  $x$  using the relation (7); we have

$$\frac{d}{d\nu} = \frac{dx}{d\nu} \frac{d}{dx} = \left[ \frac{d\nu}{dx} \right]^{-1} \frac{d}{dx} = (1-x)^2 \frac{d}{dx}. \quad (18)$$

Now the first differential equation of (14) can be written as follows:

$$\frac{dp_A}{dx} = \frac{\langle k \rangle}{(1-x)^2} \left( -2p_A^2 - 2p_{APB} - 2p_{APT} - 2p_{APP} + \frac{2}{3}p_B^2 + \frac{2}{3}2p_{BPP} \right), \quad (19)$$

and similarly for the four remaining equations, which are constructed in the same manner as (19), by replacing the right-hand side expression in the parentheses by corresponding expressions appearing in equations (14).

Let us consider the simplified version of the system valid at the onset of modifier's addition, for low values of  $x \leq 0.25$ . In this case, the system

can be linearized and solved almost immediately. The initial conditions are clear: at  $x = 0$  we have

$$p_A(0) = \frac{2}{3}, p_B(0) = \frac{1}{3}, p_{TT}(0) = 0, p_P(0) = 0, p_D(0) = 0.$$

It is also obvious that at the very beginning, the dependence of  $p_{TT}$ ,  $p_P$  on  $x$  is linear in  $x$ , while  $p_D$  can be only quadratic in  $x$ . Keeping only the powers of  $p_A$  and  $p_B$  and neglecting the  $p_{TT}$ ,  $p_P$  and  $p_D$  in the right-hand sides leads to the following approximate system at  $x$  close to 0:

$$\begin{aligned} \frac{dp_A}{dx} &\simeq \left( -2p_A^2 - 2p_{APB} + \frac{2}{3}p_B^2 \right) (2p_A + 3p_B \dots), \\ \frac{dp_B}{dx} &\simeq (-2p_B^2 - 2p_{APB} \dots) (2p_A + 3p_B \dots), \\ \frac{dp_{TT}}{dx} &\simeq \left( p_A^2 + \frac{2}{3}p_B^2 \right) (2p_A + 3p_B \dots), \\ \frac{dp_P}{dx} &\simeq \left( p_A^2 + 4p_{APB} + \frac{2}{3}p_B^2 \right) (2p_A + 3p_B \dots), \end{aligned} \quad (20)$$

We do not write down the fifth equation (for  $p_D(x)$ ), because at this stage  $p_D$  is of the order of  $x^2$ , therefore can be neglected. A further simplification can be made by taking into account the constant ratio  $p_B = p_A/2$  which should remain valid for very small amounts of alkali modifier and the fact that the rate of other reactions involving pairs of  $P$ ,  $T$  or  $D$  are negligible until the  $A$  and  $B$  configurations prevail, which remains true up to  $X = 0.2$ .

Therefore at zeroth approximation we can replace  $p_B$  by  $p_A/2$  and keep only the constant terms on the right-hand side of the differential equations (14). This yields the following approximate system in which all but constant terms have been neglected,  $p_A$  replaced by its initial value  $2/3$  and  $p_B$  by its initial value  $1/3$ :

$$\frac{dp_A}{dx} = -\frac{119}{12}p_A^3, \quad \frac{dp_B}{dx} = -\frac{63}{12}p_A^3, \quad \frac{dp_{TT}}{dx} = \frac{49}{12}p_A^3, \quad \frac{dp_P}{dx} = \frac{133}{12}p_A^3.$$

The fractions on the right-hand sides are so close to integer numbers, that we shall use the following approximation:

$$\frac{dp_A}{dx} = -10p_A^3, \quad \frac{dp_B}{dx} = -5p_A^3, \quad \frac{dp_{TT}}{dx} = 4p_A^3, \quad \frac{dp_P}{dx} = 11p_A^3, \quad (21)$$

It is easy to solve the first equation by direct integration, which gives

$$\frac{dp_A}{p_A^3} = -10dx \rightarrow p_A^{-2} = 20x + C, \quad (22)$$

C being the integration constant. At  $x = 0$  the value of  $p_A^{-2}$  is  $9/4$ , so  $C = 9/4$ , and we get the solution

$$p_A(x) = \frac{2}{3} \left( 1 + \frac{80}{9}x \right)^{-\frac{1}{2}}. \quad (23)$$

Expanding (23) around  $x = 0$  we get the following approximate solution for  $p_A(x)$  and  $p_B(x) = p_A(x)/2$  in the vicinity of  $x = 0$ :

$$p_A(x) \simeq \frac{2}{3} - \frac{80}{27}x, \quad p_B(x) \simeq \frac{1}{3} - \frac{40}{27}x, \quad (24)$$

Keeping only the constant terms on the right-hand sides of two subsequent equations we get easily

$$\frac{dp_{TT}}{dx} \simeq 4p_A^3 = \frac{96}{81}, \quad \frac{dp_P}{dx} \simeq 11p_A^3 = \frac{266}{81} \rightarrow p_{TT} \simeq \frac{96}{81}x, \quad p_P \simeq \frac{266}{81}x.$$

At this approximation stage the diborates are still “invisible”, because their number is proportional to  $x^2$  and does not appear in linear approximation.

Even at this stage of very crude approximation we can get predictions concerning the derivatives of abundance curves displayed in figure (13) at  $x = 0$ . According to the approximate linear solutions, the derivatives with respect to  $x$  at  $x = 0$  take on the following values:

$$\frac{dp_A}{dx}(0) \simeq -3, \quad \frac{dp_B}{dx}(0) \simeq -1.5, \quad \frac{dp_{TT}}{dx}(0) \simeq 1.2, \quad \frac{dp_P}{dx}(0) \simeq 3.3, \quad (25)$$

where we have used approximate values of fractions appearing in (24). The abundance of boroxol rings is evaluated as  $\frac{3}{4}p_A + p_B$  this yields the value of derivative at  $x = 0$  of the curve representing boroxol rings' abundance being equal to  $-3.85$ .

Comparing these values with the curves in (13), we see that they are in a quite fair agreement with the experimental data.

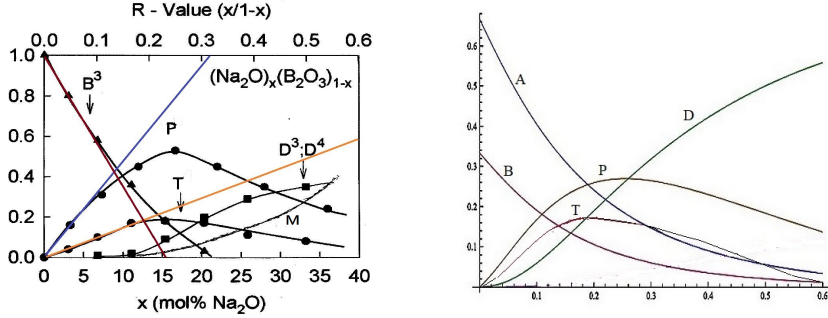


Figure 14: Left: The plot showing the relative abundance of local configurations  $P, T, D$  and  $M$  as well as the pure borate clusters  $A$  and  $B$  with linear approximations at  $x = 0$  shown with straight lines; Right: solutions of the first approximation system obtained with Maple programme. They are close enough to the experimental curves only at very low alkali concentrations ( $x \leq 0.1$ )

## 6 Rigidity and glass transition temperature

The glass transition temperature in covalent glasses depends crucially on topological properties of random network, in first place on its *connectivity*. The simplest and most compact expression of this complex statistical feature is the *average coordination number* ([2], [8], [24]), which represents a purely topological characteristic of a random network, and contains no information about forces and energies involved. Its influence on the glass transition temperature is of exclusively entropic nature. A simple rule was derived expressing the initial slope of the curve  $T_g(x)$  at working very well in covalent binary chalcogenide glasses like  $Se_xAs_{(1-x)}$  or  $As_xGe_{(1-x)}$ . If the primary glass former's atoms are  $m$ -valenced and the modifier's atoms are  $m'$ -valenced, the derivative of the glass transition temperature curve is given by the following formula:

$$\left. \frac{dT_g}{dx} \right|_{x=0} = \frac{T_g(x=0)}{\ln\left(\frac{m'}{m}\right)}. \quad (26)$$

It works perfectly well for covalent random network glasses, but much less so for oxides, in particular borates and silicates, displaying local ring structures.

A simple model of glassy thermodynamics by G.G. Naumis([32]) relates the glass transition temperature  $T_g$  with number of *floppy modes* in a given glass. The formula relating  $T_g$  with the density  $f$  of floppy modes has the

following form:

$$T_g(f) = \frac{T_g(f=0)}{1 + \alpha f}. \quad (27)$$

The density of “floppy modes” among all vibrational modes in a given glass network, although not identical with “zero frequency modes”, can be directly related to the density of broken angular constraints of bridging oxygens non involved in boroxol rings.

The formula (27) can be compared with the Gibbs-Di Marzio phenomenological formula using the average coordination number  $c$ :

$$T_g(c) = \frac{T_g(\langle c \rangle = 2)}{1 - \beta(\langle c \rangle - 2)}, \quad \beta = \frac{5\alpha}{2\alpha + 6}. \quad (28)$$

In covalent glasses, the Gibbs-Di Marzio formula applies with the value of  $\beta = 0.72$ . We may try a similar formula as function of our rigidity defect parameter  $\langle r \rangle$  as follows:

$$T_g(\langle r \rangle) = \frac{T_g^{iso}}{1 - \gamma \langle r \rangle} \quad (29)$$

The best fit for our version of  $T_g$  for alkali-borate glass is when  $\gamma = 1.45$ , close to  $2\beta$  of the Gibbs-Di Marzio formula.

At a given value of the modifier concentration  $x$  we can evaluate the average rigidity defect of the network at a given value of the modifier concentration  $x$  can be evaluated taking the mean statistical value of  $r$ :

$$\langle r \rangle = \sum_i p_i r_k, \quad \text{with } i = A, B, P, TT, D, \text{ etc.} \quad (30)$$

The values of  $r$  for particular configurations were given previously. The average rigidity defect as a function of  $x$  are given in Table II below, followed by the curve  $T_g(x)$  resulting from the dependence of  $T_g$  on  $\langle r \rangle = \langle r \rangle(x)$  given by the formula (29).

$x$	$p_A$	$p_B$	$p_P$	$p_T$	$p_D$	$p_M$	$\langle r \rangle$
0.00	0.67	0.33	0	0	0	0	-0.257
0.08	0.42	0.21	0.28	0.19	0	0	-0.161
0.15	0.267	0.136	0.43	0.17	0	0	-0.104
0.20	0.167	0.083	0.52	0.16	0.07	0.04	-0.082
0.25	0.107	0.05	0.53	0.19	0.09	0.05	-0.045
0.30	0.033	0.017	0.46	0.16	0.17	0.08	-0.094
0.35	0	0	0.43	0.17	0.22	0.18	-0.104
0.40	0	0	0.38	0.16	0.28	0.19	-0.108

Table II: Average rigidity defect  $\langle r \rangle$  for different concentrations of  $Na_2O$ .

The values calculated averaging from experimental data in (13).

We observe that alkali borate glasses  $(Na_2O)_x(B_2O_3)_{1-x}$  are *floppy* from  $x \leq 0.2$ , close to *isostatic* in the range  $0.2 < x < 0.3$  and floppy again beyond  $x > 0.3$ .

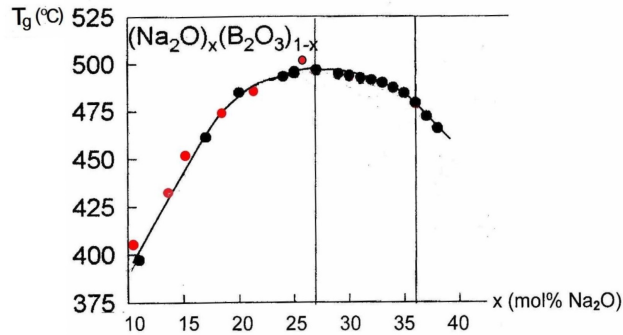


Figure 15: The glass transition temperature  $T_g$  versus  $Na_2O$  molar concentration. Black: Experiment (courtesy P. Boolchand), Red: theory (formula (29))

## Acknowledgements

One of us (R.K.) gratefully acknowledges many inspiring and fruitful discussions with Rafael Barrio, James C. Phillips, Punit Boolchand and Matthieu Micoulaut. Special thanks are due to Punit Boolchand for generous sharing his experimental results.

## References

- [1] Bray, P.J., 1985. Structural models for borate glasses. *Journal of Non-Crystalline Solids*, **75** (1-3), pp.29-36
- [2] R. Kerner, 1991 A model for formation and structural properties of alkali borate glasses, *Journal of Non-Crystalline Solids*, **135** 155-170.
- [3] Barrio, R. A., Castillo-Alvarado, F.L. and Galeener F.L., Structural and vibrational model for vitreous boron oxide *Physical Review B*, 1991 **44**, 7313.
- [4] Massot, M. and Balkanski, M., 1992 in *Microionics, Solid State Integrate Batteries* (M. Balkanski editor), North Holland, p.135
- [5] Barrio R.A., Duruisseau J-P. and Kerner R, 1995 Structural properties of alkali-borate glasses derived from a theoretical model, *Phil. Magazine* **B 72** (5), 535-550.
- [6] Micoulaut, M., Kerner, R. and dos Santos-Loff, D.-M. 1995 Statistical modelling of structural and thermodynamical properties of vitreous  $B_2O_3$  *Journ. of Phys. Cond.Matter* **7**, 8035. *ibid*, **31**, 323-331.
- [7] Barrio, R.A., Kerner, R., Micoulaut, M. and Naumis, G.G. 1997. Evaluation of the concentration of boroxol rings in vitreous by the stochastic matrix method. *Journal of Physics: Condensed Matter*, **9** (43), 9219
- [8] Kerner, R., Two simple rules for covalent binary glasses 1995 *Physica B: Condensed Matter* **215** (2-3), 267-272
- [9] Kerner, R and Micoulaut, M. On the glass transition temperature in covalent glasses 1997 *Journal of non-crystalline solids* **210** (2-3), 298-305
- [10] Wright, A.C., Vedishcheva, N.M. and Shakhmatkin, B.A., 1995 Vitreous borate networks containing superstructural units: a challenge to the random network theory?. *Journal of non-crystalline solids*, **192**, pp.92-97.
- [11] Krogh-Moe, J. J., 1969. The structure of vitreous and liquid boron oxide. *Journal of Non-Crystalline Solids*, **1** (4), 269-284
- [12] Bray, P.J., Feller, S.A., Jellison Jr, G.E. and Yun, Y.H., 1980 B10 NMR studies of the structure of borate glasses 1980 *Journal of Non-Crystalline Solids*, **38**, 93-98
- [13] Gibbs, J.H. and Di Marzio, E.A. 1958 Nature of the glass transition and the glassy state *Journal of Chemical Physics*, **28** p. 373



- [14] Hannon, A.C., Grimley, D.I., Hulme, R.A., Wright, A.C. and Sinclair, R.N. 1994 Boroxol groups in vitreous boron oxide: new evidence from neutron diffraction and inelastic neutron scattering studies. *Journal of non-crystalline solids*, **177**, pp.299-316.
- [15] Walrafen G. E., Samanta S. R., Krishnan P.N., 1980 Raman investigation of vitreous and molten boric oxide. *J. Chem. Phys.*, p. 113-120
- [16] Galeener, F.L., Barrio, R.A., Martinez, E. and Elliott, R.J. 1984 Vibrational decoupling of rings in amorphous solids. *Phys. Rev. Letters*, **53** (25), 2429
- [17] Krogh-Moe, J., 1963 Energy and Length of the Boron-Oxygen Bond. *Acta Chemica Scandinavica*, **17**, 843-864
- [18] Kerner, R and dos Santos, D.-M., 1988 Nucleation and amorphous and crystalline growth: A dynamical model in two dimensions *Physical Review B* **34** 858-878.
- [19] A.C. Wright and N.M. Vedishcheva, *European Journal of Glass Science and Technology B*, **57** (1), 1-14 (2016)
- [20] G. E. Jellison, G.E., L.W. Panek, L.W., P.J. Bray, P.J. and Rouse, G.B., 1977 Determinations of structure and bonding in vitreous  $B_2O_3$  by means of  $B_{10}$ ,  $B_{11}$ , and  $O_{17}$  NMR *Journal of Chemical Physics*, **66**, p.802.
- [21] Hannon, A.C., Sinclair, R.N. and A.C. Wright, A.C. 1993 The vibrational modes of vitreous  $B_2O_3$  , *Physica A*, **201**, p. 373
- [22] Wright, A.C., Vedishcheva, N.M. and Shakhmatkin, B.A., 1996 A crystallographic guide to the structure of borate glasses. *MRS Online Proceedings Library* (OPL), 455.
- [23] Ferlat G. *et al.*, 2008 Boroxol Rings in Liquid and Vitreous  $B_2O_3$  from First Principles, *Phys. Rev. Letters*, **101**, 065504.
- [24] Kerner, R. Models of Agglomeration and Glass Transition, (book), 2007 *Imperial College Press*.
- [25] Wright, A.C., Vedishcheva, N.M. and Shakhmatkin, B.A. *Mat. Res. Soc. Symp. Proceedings*, **455** 381 (1997).
- [26] Mauro, J.C., Gupta, P.K. and Loucks, R.J. 2009 Composition dependence of glass transition temperature and fragility. II. A topological model of alkali borate liquids. *Journal of chemical physics*, **130** (23):234503.

- [27] Jellison, G.E. and Bray, P.J., 1978 A structural interpretation of  $B^{10}$  and  $B^{11}$  NMR spectra in sodium borate glasses, *Journal of Non-Crystalline Solids*, **29**, pp. 187-206 (1978).
- [28] Phillips J.C. and Kerner, R. 2008 Structure and function of window glass and Pyrex *J. Chem. Phys.* **128**, 174506
- [29] Vignarooban, K., Boolchand, P., Micoulaut, M., Malki, M. and Bresser, W. 2014 Rigidity transitions in glasses driven by changes in network dimensionality and structural groupings *Europhysics Letters*, **108**, 56001
- [30] Vignarooban, K., 2012 Ph. D. thesis "Boson mode, dimensional crossover, medium range structure and intermediate phase in Lithium- and Sodium-borate glasses", *University of Cincinnati*.
- [31] Dove, M.T., Harris, M.J., Hannon, A.C., Parker, J.M., Swainson, I.P. and Gambhir, M., 1997 Floppy modes in crystalline and amorphous silicates. *Physical Review Letters*, **78** (6), p.1070.
- [32] Naumis, G.G. 2006 Variation of the glass transition temperature with rigidity and chemical composition *Physical Review B*. **73** (17):172202.